



1 Using single remote sensing image to calculate the height of the
2 landslide dam and the maximum volume of the lake

3

4 Weijie Zou ^{1,2}, Yi Zhou ¹, Shixin Wang ¹, Futao Wang ¹, Litao Wang ¹, Qing
5 Zhao ¹, Wenliang Liu ¹, Jinfeng Zhu ¹, Yibing Xiong ^{1,2}, Zhenqing Wang ^{1,2},
6 Gang Qin ^{1,2}

7 ¹Aerospace Information Research Institute, Chinese Academy of Sciences, Beijing, 100094, China;

8 ²University of Chinese Academy of Sciences, Beijing 100049, China;

9 Correspondence: Yi Zhou (zhouyi@radi.ac.cn) and Futao Wang (wangft@aircas.ac.cn)

10 **1. Abstract**

11 Landslide dams are caused by landslide materials blocking rivers. After the occurrence of large-scale
12 landslides, it is necessary to conduct large-scale investigation of barrier lakes and rapid risk assessment.
13 Remote sensing is an important means to achieve this goal. However, at present remote sensing is only
14 used for monitoring and extraction of hydrological parameters at present, without prediction on potential
15 hazard of the landslide dam. The key parameters of the barrier dam, such as the dam height and the
16 maximum volume, still need to be obtained based on field investigation, which is time-consuming. Our
17 research proposes a procedure that is able to calculate the height of the landslide dam and the maximum
18 volume of the barrier lake, using single remote sensing image and pre-landslide DEM. The procedure
19 includes four modules: (a) determining the elevation of the lake level, (b) determining the elevation of
20 the bottom of the dam, (c) calculating the highest height of the dam, (d) predicting the lowest crest height
21 of the dam and the maximum volume. Finally, the sensitivity analysis of the parameters during the
22 procedure and the analysis of the influence of different resolution images is carried out. This procedure
23 is demonstrated through Baige Landslide Dam in south-west China. The single image from Beijing-1
24 and pre-landslide DEM, SRTM V3, are used to predict the height of the dam and the key parameters of
25 the dam break, which are in good agreement with the measured data. This procedure can effectively
26 support the quick decision-making regarding hazard mitigation.

27

28 Keywords: Landslide dam, Remote sensing, DEM, Dam height, Hazard



29 **2. Introduction**

30 Landslide dams are caused by landslide materials blocking rivers, usually in mountainous areas with
31 rivers and narrow valleys, bringing great risks to local people's lives and property(Costa and Schuster,
32 1988; Fan et al., 2020). Landslide dams disaster is widely distributed around the world. For instance, the
33 11 dams caused by the Magnitude 7.6 earthquake in New Zealand 1929(Adams, 1981); Oso Landslide
34 Dam in Washington, USA in 2014(Iverson et al., 2015); Diexi Landslide Dam on Minjiang River, China,
35 1933(Li et al., 1986); Yigong Landslide Dam in 2000(Zhou et al., 2016) and a series of landslide dams
36 including the Tangjiashan Landslide Dam caused by the Wenchuan earthquake in 2008(Zhang et al.,
37 2019).

38 Based on the historical records of 183 landslide dams, Costa found that the main way of dam breaching
39 was overtopping. 41% of dams breached within one week, and 85% breached within a year(Costa and
40 Schuster, 1988). Respectively Fan analyzed a series of dams induced by the 2008 Wenchuan earthquake
41 finding that 43% of them collapsed within one month(Fan et al., 2012). And according to Shen's research
42 on the longevity of the barrier lake, nearly 48.3% of the dams will breach within a week, and 84.4% of
43 the dams will fail within one year(Shen et al., 2020). Generally speaking, landslide dams are unstable.
44 However, the landslide dam always occurred in remote mountainous areas, with inconvenient traffic
45 conditions and poor infrastructure(Cui et al., 2009). When earthquakes or precipitation induce large-scale
46 landslides, field survey is time-consuming and manpower-consuming(Dong et al., 2014). Remote areas
47 tend to be more vulnerable and the dam breaching are more likely to cause serious consequences. So, it
48 requires us to identify the landslide dam and take action as quickly as possible.

49 Remote sensing has the ability to identify and monitor landslide dams on a large scale conveniently, and
50 can support quick decision-making regarding hazard mitigation(Canutì et al., 2004; Fan et al., 2021). In
51 the research before, remote sensing is usually regarded as an auxiliary means to monitor the change of
52 the catchment area or to measure the length of the dam. For example, Wang and Lv used multiple remote
53 sensing images to extract water boundary images and pre-landslide DEM to monitor the changes of lake
54 volume of Yigong Lake(Wang and Lu, 2002). Respectively, Cheng et al. proposed a method to estimate
55 reservoir capacity of water based on water boundary and DEM(Chen and Lu, 2008).

56 The researches above focused on obtaining information of the barrier lake through remote sensing and
57 Geographic Information System. However, these kinds of methods focus on monitoring and lack
58 judgment of future development of the landslide dam. Some essential components of hazard evaluation
59 are not available in these researches. Especially the height of the dam which determines the maximum
60 volume of the barrier lake and the flood peak of the dam breaching(Costa and Schuster, 1988; Ermini
61 and Casagli, 2003; Peng and Zhang, 2012; Dong et al., 2014) can't be obtained through these methods.

62 With the rapid development of Unmanned Aerial Vehicles (UAVs), in 2008, photogrammetric UAVS are
63 also used to survey the landslide dams in the Wenchuan earthquake in 2008(Cui et al., 2009). However,
64 after the earthquake, there are to be a large number of landslides and the affected area is considerably
65 huge. If UAVs are used for precise investigation one by one, it cannot meet the requirements of timeliness

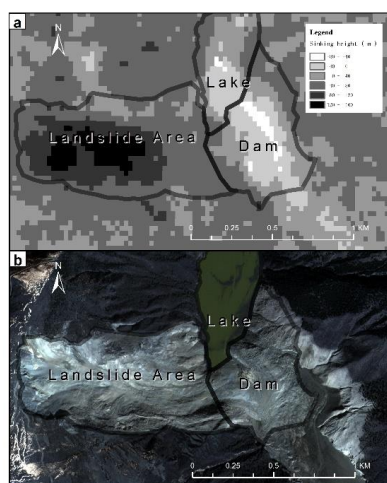


66 for the emergency. Based on the pre-landslide DTM and a series of remote sensing images after the
67 landslide dam, Dong obtains the variation of the lake level to estimate the slope foot of the barrier dam
68 and predict the dam height, completing quickly assessment of the dam breaching hazard(Dong et al.,
69 2014). But this procedure is still inconvenient as it requires sequential images to predict the height of the
70 dam.

71 What's more, all of the methods that use the pre-landslide DEM are based on an important assumption
72 that the pre-landslide DEM is reliable. Nevertheless, take Baige Landslide Dam as example (Fig 1), we
73 can find that the elevation of landslide area changes greatly. The landslide area has a greater degree of
74 subsidence, and the dam area has a greater degree of uplift. And even in areas nearby covered with
75 vegetation, there was about 20 meters of subsidence averagely, which demonstrates that the assumption
76 above need further improvement.

77 This research will focus on the weakness above using single remote sensing image and pre-landslide
78 DEM to obtain the essential information of the landslide dam and calculating the height of the landslide
79 dam based on the formation mechanism of the landslide dam. The Baige Landslide Dam is taken as an
80 example to verify the feasibility of this procedure. And the sensitivity analysis of the parameters during
81 the procedure and the analysis of the influence of different image resolution will be carried out in the
82 discussion part.

83

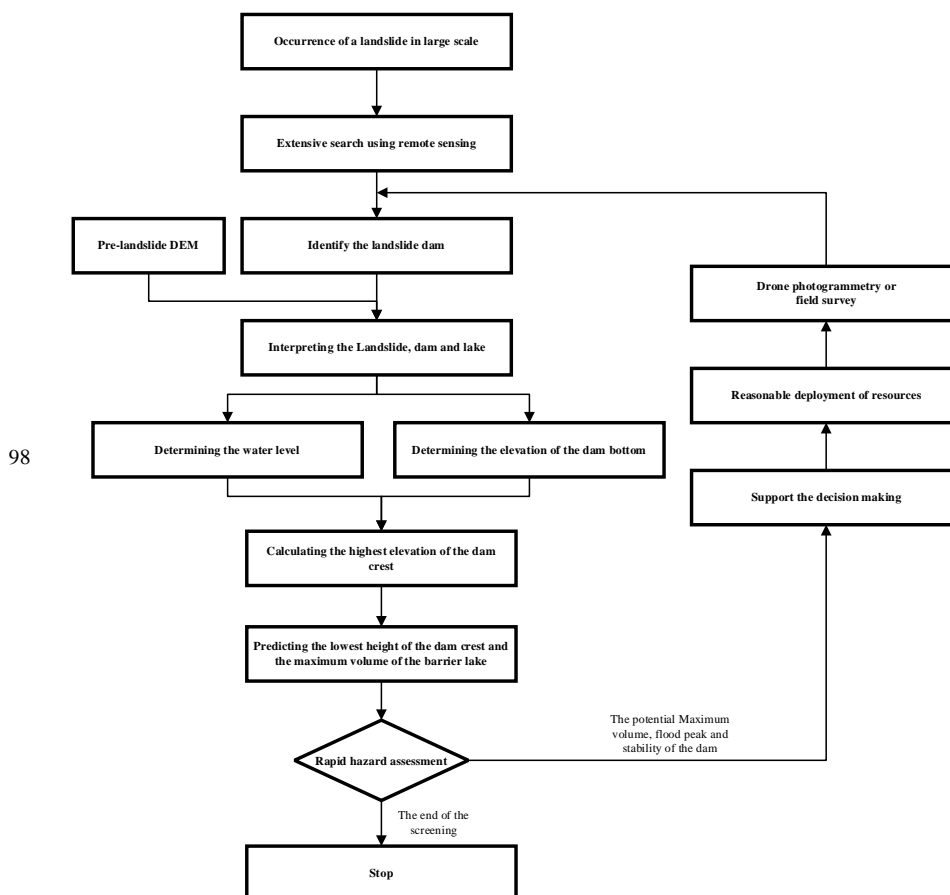


84 Fig 1 picture a is the comparison of pre-landslide DEM (SRTM V3) and the after-landslide Dem. And
85 picture b is the remote sensing image from Beijing-1 satellite (taken in November 9, 2018)



86 3. Procedure

87 After the occurrence of large-scale landslides, the government often can't get all the disaster situation
88 immediately, so large-scale landslides investigation is needed. As the disaster often occurs in remote
89 areas, the purpose of the large-scale investigation is not only to find the landslide dams, but also to make
90 an objective evaluation of the hazard of the landslide dams, supporting reasonable allocation of resources
91 to avoid excessive reaction. When a landslide dam is identified from the image, the procedure to calculate
92 its height is divided into four parts: (a) selecting the reference points to determine the elevation of the
93 lake level; (b) estimating the elevation of the bottom of the dam; (c) calculating the highest elevation of
94 the dam crest based on the formation mechanism of the landslide dam; (d) predicting the lowest height
95 of the dam crest and the maximum of the lake volume. This section will elaborate the details of (a), (b),
96 (c) and (d), obtaining the lowest height of the dam crest and calculating the maximum volume based on
97 GIS.





99

100 Fig 2 the procedure of obtaining the height of the dam crest and completing the hazard assessment

101 3.1. Determining the elevation of the lake level

102 The method of estimating the elevation of the barrier lake based on remote sensing images has been
103 practiced by many scholars. Typically speaking, researchers assume that the elevation of the water
104 boundary is the same as the topography. And pre-landslide DEM is used in most cases to determine the
105 lake level with the water boundary in the image(Wang and Lu, 2002; Chen and Lu, 2008; Dong et al.,
106 2014; Braun et al., 2018). However, the reliability of the pre-landslide DEM may decrease as a result of
107 landslides (Fig 1). The reasons are summarized as follows: (a) the landslide has caused some changes in
108 the topography of the area; (b) the pre-landslide DEM has errors itself, especially in the mountainous
109 area; (c) as the pre-landslide DEM usually can not be undated in time, there can be some landslides
110 without records before.

111 For the reasons above, the selection of the reference points to determine the elevation of the lake level
112 should follow these principles to reduce errors. (a) As landslides often bring about large-scale ground
113 subsidence, when selecting reference points, the point around the landslide area should be avoided. (b)
114 Because landslides and settlements tend to occur in areas with steep terrain and little vegetation
115 coverage(Ayalew and Yamagishi, 2005) and the DEM is more precise in flat terrain, the reference points
116 should be in vegetation-covered flat terrain, avoiding gully or ravines.

117 Under these strictions the reference points selected can be regarded as having the same elevation of the
118 lake level. Therefore, the lake level is determined. However, in order to determine the elevation of the
119 lake level, a complex number of reference points are needed. Their value can't be the same for the random
120 errors but should be within a certain range(Fig 6), for the random errors of DEM and the errors in the
121 process of determining the points. In this situation, points that are one and a half interquartile range away
122 from the mean value are considered outliers. And the elevation of the lake level is the average elevation
123 of the remains. Because the dam blocks the channel and the river has no outflow, the water surface can
124 be assumed to be still(Wang and Lu, 2002; Morgenstern et al., 2021; Fan et al., 2021). So, the elevation
125 of the lake level is the same as the elevation of the dam-lake point in Fig 3.

126 3.2. Determining the elevation of the dam bottom

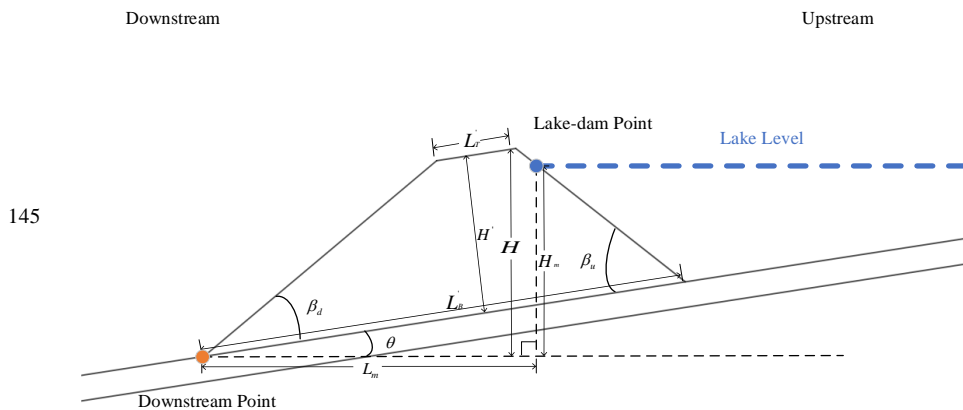
127 In this procedure, the bottom of the dam refers to the point where the dam meets the river bed on the
128 downstream side. In practical cases, the most reliable method is to directly use the riverbed elevation
129 obtained recently. In the absence of relevant data, the following method should be taken for prediction.
130 Within a certain range, the riverbed elevation can be considered to decrease in proportion along the
131 channel, conforming to a linear variation. Therefore, sampling elevation points at the lowest point of the
132 river valley in the pre-landslide DEM, removing the outliers and carrying out simple regression to obtain
133 the fitting of the riverbed elevation. By extending the fitting results to the dam body and subtracting the



134 historical river depth, the bottom elevation of the dam is obtained.
 135 However, the historical river depth is to vary with the seasons. So there must be some errors in this
 136 prediction. The influence of dam bottom elevation on calculating dam height will be analyzed in the
 137 “discussion” section.

138 3.3. Calculating the highest elevation of the dam crest

139 According to Wu's laboratory experimental study, the geometrical form of the barrier dam is mainly
 140 determined by landslide slope, river slope, angle of repose, earthwork amount and sliding height. I (Wu
 141 et al., 2020).
 142 With his theory, if the river is completely blocked and the valley can be simplified into U-shape, the
 143 longitudinal section of the landslide dam can be simplified as a trapezoid(Wu et al., 2020). And the
 144 trapezoid will follow the following pattern.



146 Fig 3 simplified section of the landslide dam

147 The top of the dam is parallel to the bottom of the dam (Wu et al., 2020).

$$148 \quad L_T \parallel L_B \quad (1)$$

149 Where L_T is the top of the dam, L_B is the bottom of the dam (Wu et al., 2020).

$$150 \quad \beta_d + \theta = \beta_u - \theta = \chi\varphi \quad (2)$$

151 Where β_d is the angle between the body of the dam and the riverbed on the downstream side, β_u is
 152 the angle between the body of the dam and the riverbed on the upstream side, φ is the angle of repose
 153 of the landslide mass and χ is the parameter that fits the effect of “cut top” phenomenon. φ is
 154 determined by the nature of the soil itself and χ will be affected by landslide surface angle, landslide
 155 length and other factors(Grasselli et al., 2000). The determining of the χ can be simplified as
 156 follows(Wu et al., 2020):

$$157 \quad \chi = 0.57 + 0.51 \left(1 + e^{\frac{(\alpha-34)}{10.50}} \right)^{-1} \quad (3)$$



158 where α is the angle of the landslide surface. As the angle is higher, the actual angle between the
159 riverbed and the landslide material will be smaller and the length of the dam along the river will be longer.
160 Normally speaking, this formula fits the actual situation well. The precise of this fitting will be discussed
161 in the “discussion” section.

162 According to Wang's field investigation on the Wenchuan earthquake, it is found that the angle of repose
163 of landslide dam in the Wenchuan earthquake is between 28.8° and 44.7° , with an average of 35.5° (Wang
164 et al., 2013). In the absence of relevant data, it is recommended to use the average provided by Wang.

$$165 \varphi = 35.5^\circ \quad (4)$$

166 Wu proposed that the height of the dam has a certain relationship with the length of the bottom of the
167 dam (Wu et al., 2020), as follows:

$$168 H' = (0.37 + 1.1 \tan \theta) \cdot \tan(\beta_d + \theta) \cdot L_B' \quad (5)$$

169 where H' is the height between the dam top and the dam bottom, θ is the angle of the riverbed and

170 L_B' is the length of the dam along the river. The R^2 of formula (1) (2) (3) (5) are all greater than 0.95.

171 As shown in Fig 3, the elevation of the dam-lake point and the elevation of the dam bottom has already
172 been obtained before. So, H_m can be calculated and L_m can be obtained directly from the remote
173 sensing images. According to formula (1), (2), (3), (4) and (5), using simple geometric relations, the
174 following relation can be obtained:

$$175 L_B = \frac{L_m}{\cos \theta} + \frac{\cos(\beta_u - \theta)}{\sin \beta_u} \cdot (H_m - L_m \cdot \tan \theta) \quad (6)$$

$$176 H = \frac{H'}{\cos \theta} + \sin \theta \cdot (L_B - H' \cdot \tan \theta - H' \cdot \tan(90 - \beta_u)) \quad (7)$$

177 Where H is the difference between the highest elevation of the dam crest and the dam bottom
178 elevation. θ and α can be obtained through the remote sensing image and the pre-landslide DEM easily.

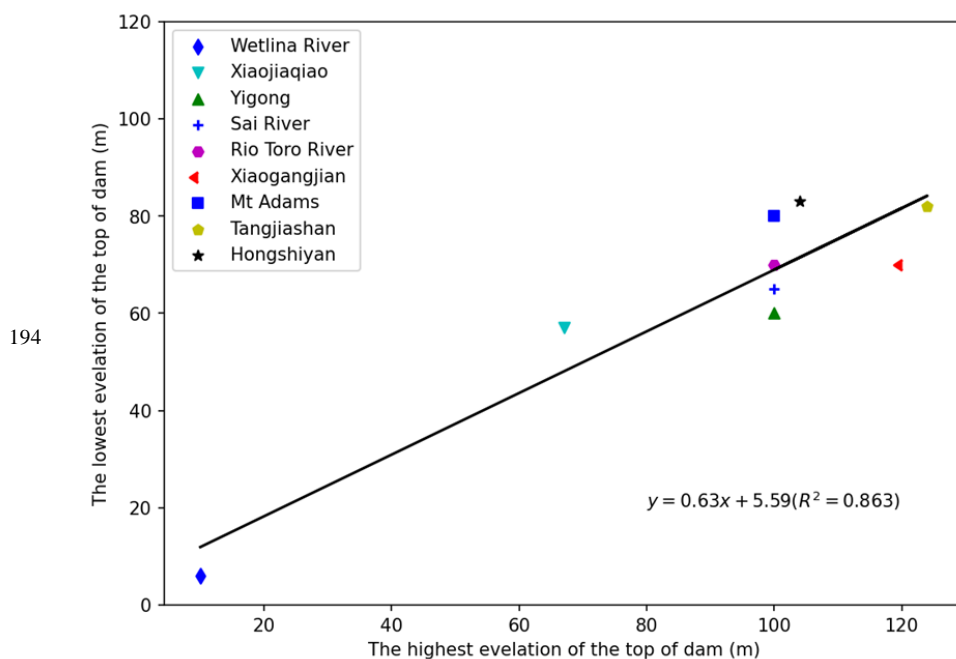
179 Through this procedure, the highest elevation of dam crest is determined based on a single image and
180 pre-landslide DEM, which can be used in the further prediction of the dam breaching and related
181 decision-making.

182 3.4. Predicting the lowest height of the dam crest and the 183 maximum volume of the barrier lake

184 Because the height of the landslide dam in the vertical direction of the river channel will not be
185 consistent (Costa and Schuster, 1988; Fan et al., 2020), but will form different types of distribution
186 according to the characteristics of the case, resulting in the height of the landslide dam is not a simple
187 value but a range. As the most important factor affecting the dam break of a barrier lake is the height of
188 the lowest point of the dam crest, which determines the potential maximum volume of the barrier lake
189 and the maximum discharge volume of the dam breach (Costa and Schuster, 1988; Chen et al., 2004, 2021;



190 Dong et al., 2011, 2014; Yang et al., 2013; Zhong et al., 2018), the prediction result of the highest
191 elevation of the dam crest can't be used in related breaching models directly.
192 But by simply analyzing the highest elevation of the dam crest and the lowest elevation in the existing
193 records, a simple estimation of the relationship between them is carried out, as shown in Fig 4.



195 Fig 4 the relationship between the highest elevation of the dam crest and the lowest elevation of the
196 dam crest. These dates come from the papers of Cui, Costa, Mora and so on(Costa and Schuster, 1991;
197 Mora Castro, 1993; Briaud, 2008; Cui et al., 2009; Peng and Zhang, 2012; Chen et al., 2020).

198 .
199 The relationship can be expressed as follows:

$$200 H_1 = 0.63H_h + 5.59(R^2 = 0.863) \quad (8)$$

201 where H_1 is the lowest elevation of the dam crest and H_h is the highest elevation of the dam crest.

202 On the basis of the formula above, we can use this procedure to complete the rapid assessment of the
203 breaching hazard.

204



205 **4. Validation of the proposed procedure**

206 **4.1. Baige Landslide Dam**

207 The Jinsha River, the upper reach of the Yangtze River, was dammed twice recently at Baige, Tibet, one
208 on 10 October 2018 and the other on 3 November 2018 (UTC+8), at $98^{\circ}42'32.24''\text{E}$, $31^{\circ}4'59.27''\text{N}$ (Fig
209 4) (Zhang et al., 2019) and one on November 3, 2018, the residual landslide of "10.10" Baige Landslide
210 Dam slid down again, forming "11.03" Baige Landslide Dam on the basis of the original residual dam(Li
211 et al., 2019). The dam is much larger than the first one, as the width of the dam top is 195 m, the length
212 of the dam top is 273 m and the highest elevation of the dam crest is 3014m(Chen et al., 2020). After
213 proper treatment, its storage capacity is reduced from $8.69 \times 10^8 m^3$ to $5.79 \times 10^8 m^3$ and the flood
214 peak is diminished from $41624 m^3 / s$ to $31000 m^3 / s$ (Chen et al., 2020; Yunjian et al., 2021). A
215 large number of roads and bridges were damaged downstream, and a total of 54,000 people were affected,
216 with economic loss of over 7.43 billion yuan(Zhang et al., 2019). Due to abundant field survey data and
217 its great harm, Baige Landslide Dam was selected to demonstrate this procedure.

218 Baige Landslide Dam occurred in a deep valley of the mountainous area and the barrier lake is long and
219 narrow (Fig 5). To demonstrate the proposed procedure, the image used is a 0.8m resolution image from
220 Beijing-1 which was taken on November 9, 2018 and the pre-landslide DEM we choose is SRTM V3 of
221 30m resolution which was taken in 2000. The effect of the resolution of the image will be discussed in
222 the "Discussion" section.

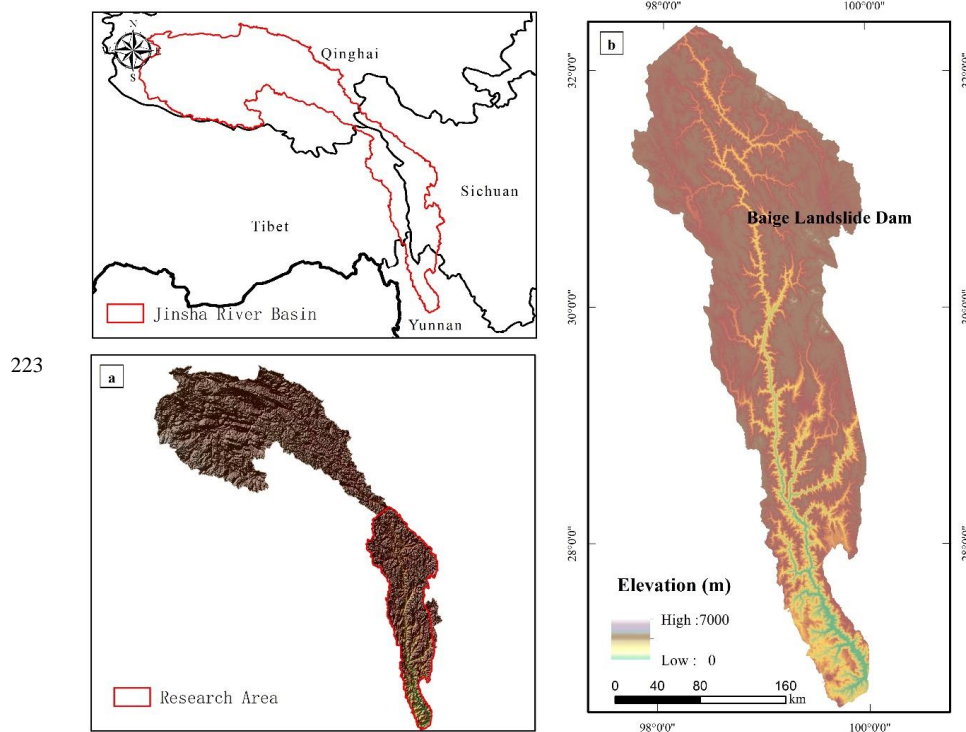


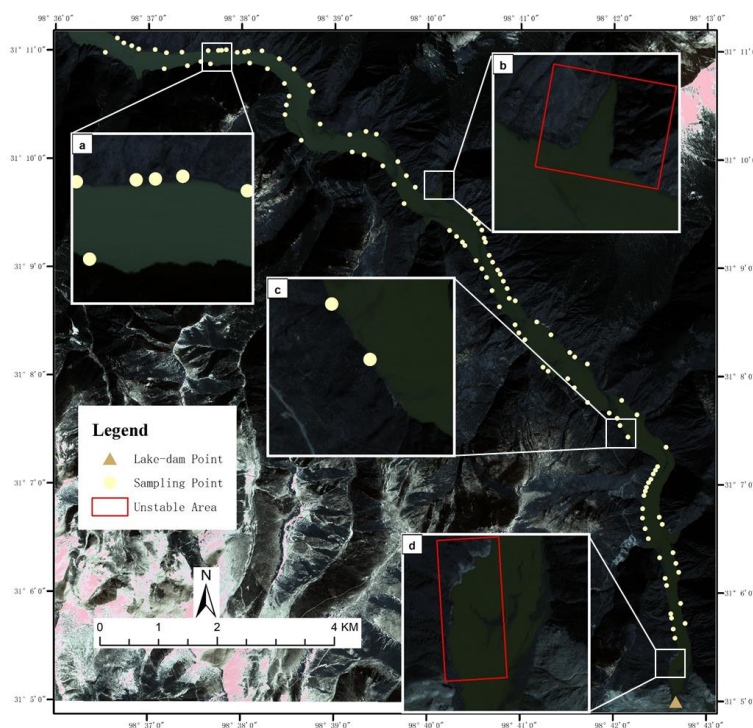
Fig 5 the position of the Baige Landslide Dam

4.2. Determine the elevation of the lake level

226 At the water boundary in the remote sensing image, the area covered by vegetation with relatively flat
227 terrain and a certain distance from the landslide was selected for elevation sampling (Fig 6). Under ideal
228 circumstances, the distribution of sampling points' elevation should be completely consistent. But in
229 practice, there are often large deviations, shown in Fig 7, the specific reasons for which have been
230 discussed in the "Procedure" section and will not be repeated. The deviation between the maximum and
231 minimum elevation of sampling points can reach 72m, and the shape basically conforms to the normal
232 distribution. Therefore, the mean of reference points can be obtained directly after clearing the outliers,
233 which is the elevation of barrier lake and the outcome is 2944m. Since the lake is essentially still, the
234 elevation of the lake should be the same as the elevation of the point where the dam meets the lake,
235 shown as the triangle in Fig 6.

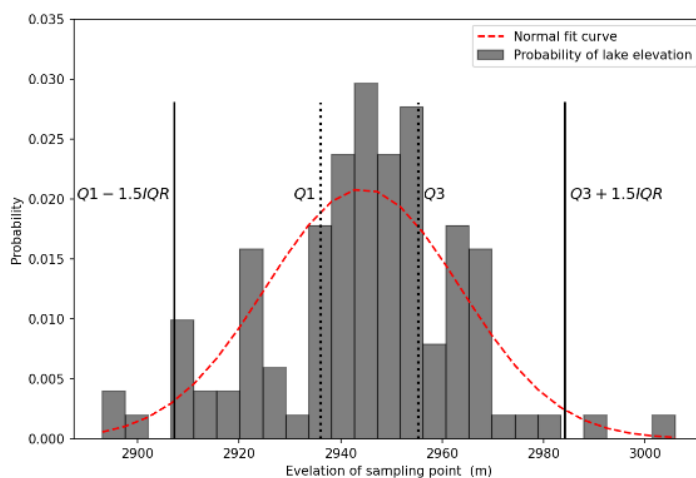


236



237 Fig 6 the sampling points in the case of Baige Landslide Dam (image from Beijing-1 satellite)

238

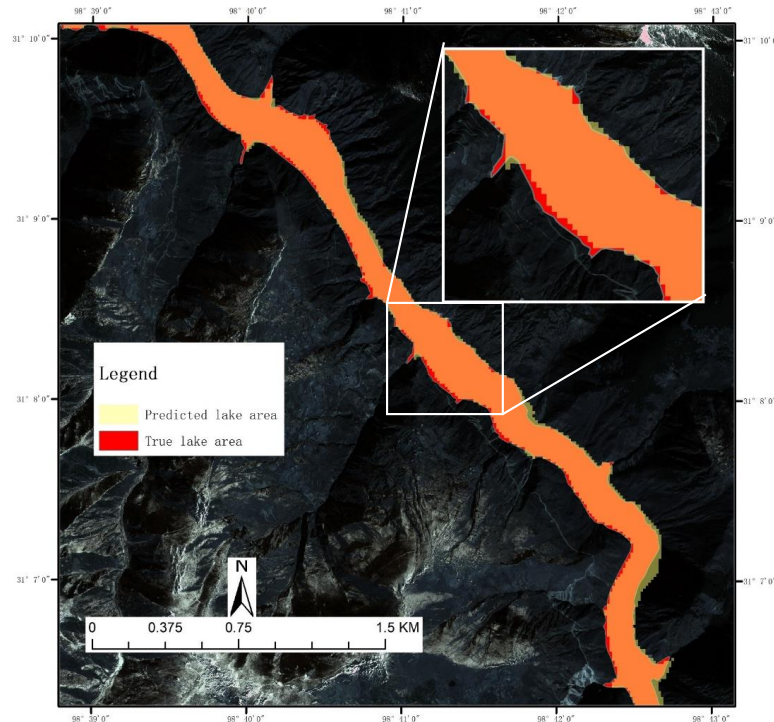


239 Fig 7 elevation distribution of sampling points

240 The Intersection over Union (IOU) of the area with elevation below 2944m in DEM and the actual
 241 submerged area in the remote sensing image is 84.48% (Fig 8). The two are found to be basically
 242 consistent.



243



244 Fig 8 the comparison of the area with elevation below 2944m in DEM and the actual submerged area in
245 the remote sensing image (image from Beijing-1 satellite)

246

247

248

249 4.3. Determining the elevation of the dam bottom

250 The inclination angle of the riverbed is calculated by sampling and unitary regression and is about 0.11° .

251 The elevation of the water level on the place of dam bottom before the landslide is 2867m. As the water
252 depth is not considered when obtaining DEM and varies with change of rainfall in the rainy season and
253 dry season, this value can't be used directly. According to the data in China Ministry of Water Resources
254 Information Center, the water depth of Jinsha River section is about 2-10m. The water depth can be
255 assumed as the mean value, 6m. Therefore, the final estimate of the dam bottom elevation is 2861m.
256 Respectively, according to the field survey, the riverbed elevation is 2860m(Chen et al., 2020).

257



258 4.4. Calculating the highest height of the dam crest

259 The slope angle of the landslide surface, the inclination angle of the riverbed and the length of the
260 landslide can be calculated directly through remote sensing image and DEM. The slope angle of landslide
261 surface is 30.65° . The inclination angle of the riverbed is 0.11° . And the length of the landslide that can
262 be observed is 567m. According to formula (5) (6) (7), with the parameters obtained before, the highest
263 height of the dam top is 155.4m and the highest elevation of the dam top is 3016.5m with an error of
264 2.5m compared to the measured data by Chen, 3014m(Chen et al., 2020).

265 4.5. Predicting the lowest height of the dam crest and the 266 maximum volume of the barrier lake

267 Taking Baige Landslide Dam as an example, according to the case section, we have predicted that the
268 highest elevation of the dam crest is 3016.5m and the height of the dam is 155.4m. According to formula
269 (8), we calculated that the lowest height of the crest of the landslide dam is 104.2m, and the elevation is
270 2964.2m with an error of 2.8m compared to the measured data by Chen, 2067m(Chen et al., 2020). Using
271 Geographic Information System, we can estimate based on DEM(Wang and Lu, 2002; Chen and Lu,
272 2008) that its potential maximum volume is $7.96 \times 10^8 (m^3)$.

273 5. Discussion

274 5.1. Rapid hazard assessment

275 The lowest height of the dam crest and the maximum volume of the barrier lake are important input
276 parameters for the dam-breaking model . This paper has given the procedure to obtain them rapidly. In
277 the simple prediction formula (9) proposed by Cenderelli., V is the maximum volume of the dammed
278 lake, and Q is the maximum flood peak of dam breaching. Without treatment, the largest flood peak of
279 the Baige Landslide Dam breaching will reach $42257 (m^3 / s)$.

280

$$281 \quad Q = 3.4 \cdot V^{0.46} \quad (9)$$

282 The comparison between the predicted result and the measured date, as shown in table 1, achieves a good
283 agreement. The rapid assessment of the dam breaching hazard has been completed. As the simulation



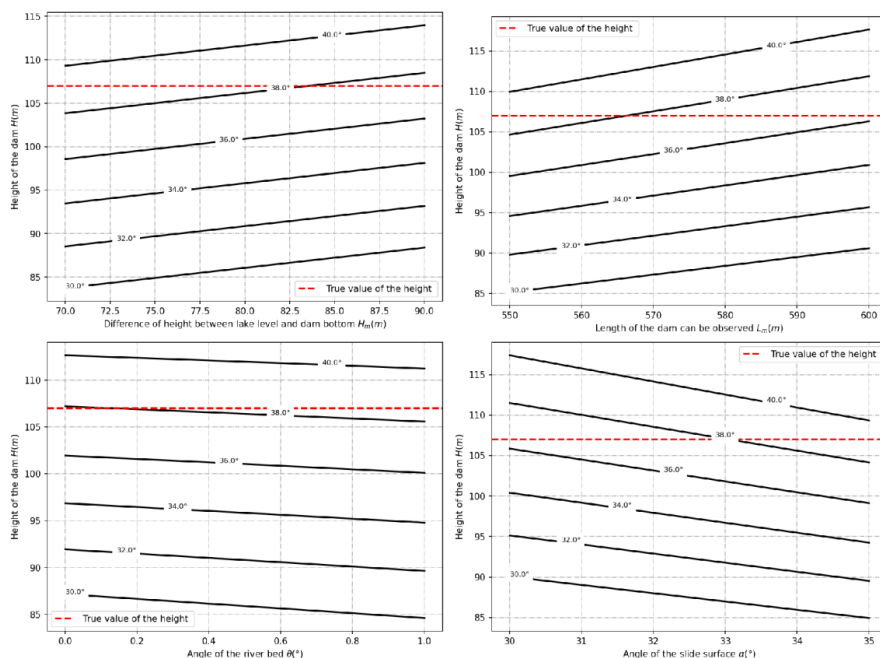
284 model of dam breaching has a significant influence on the prediction of flood peak, they should also be
285 selected carefully in practical applications. Besides Cenderelli's formula, there are also many other
286 formulas to choose to predict the dam breaching(Costa and Schuster, 1991; Walder and OConnor, 1997;
287 Shi et al., 2014; Ruan et al., 2021; Peng and Zhang, 2012; Zhong et al., 2018). And many scholars have
288 discussed the merits and demerits between these hazard assessment models(Peng and Zhang, 2012; Fan
289 et al., 2021).

Parameter	Measured data	The present method
the highest elevation of the dam top	3014 (<i>m</i>)	3016.5(<i>m</i>)
the lowest elevation of the dam top	2967 (<i>m</i>)	2964.2(<i>m</i>)
the maximum of lake volume	$8.69 \times 10^8 (m^3)^*$	$7.96 \times 10^8 (m^3)$
the peak discharge	$41624 (m^3 / s)^*$	$42257 (m^3 / s)$

290 Table 1 the comparison of the measured data and the predicted result. As relative measures have been
291 taken to reduce the maximum volume of the barrier lake, data with star in the table is the estimation
292 results of Chen's detailed back analyses(Chen et al., 2020).

293 5.2. Sensitivity analysis

294 In this procedure, the main parameters include: the length of the dam that can be observed, the elevation
295 of the lake level, the elevation of the dam bottom, the slope angle of landslide surface and the inclination
296 angle of the riverbed. Since H_m is the lake level elevation minus the elevation of the dam bottom,
297 sensitivity analysis of these two parameters will be conducted on H_m directly. The variation of the
298 prediction result with the change of parameters is shown as follows:



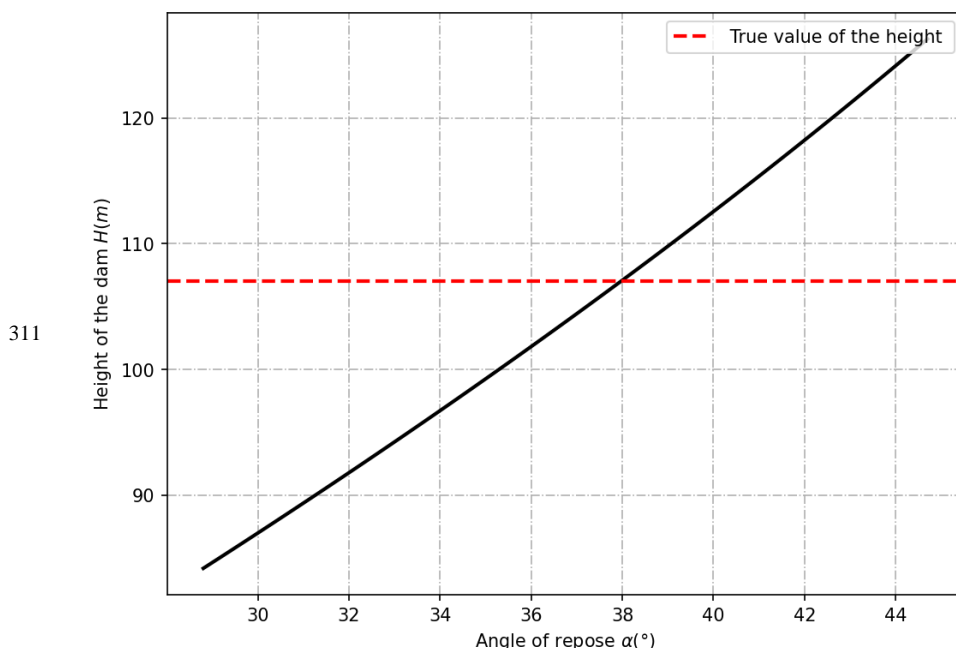
299

300 Fig 9 the relationship between the predicted result and the input parameters.

301

302 As can be seen from Fig 9, with other parameters unchanged, the greater the observable length of the
 303 dam and the difference of height between the lake level and dam bottom, the higher the dam crest. The
 304 crest of the dam gets lower as the slope angle of landslide surface and the inclination angle of the riverbed
 305 rise. The slope foot of the dam is mainly affected by the angle of landslide surface and inclination angle
 306 of the riverbed. The smaller the slope foot, the smaller the height of the dam. The calculated results are
 307 in good agreement with expectations.

308 Meantime, it can be found that these parameters all have an impact of about 10% on the final prediction
 309 results. So, it is necessary to be careful to determine these parameters. Possible methods to reduce errors
 310 include repeat procedures and more reliable historical data.



312 Fig 10 the relationship between the predicted result and the angle of repose.

313

314 Finally, it is found that the angle of repose of the dam body has a significant influence on the height of
315 the dam (Fig 10). The greater the angle of repose, the greater the estimate of dam height. According to
316 Wang's field survey, the angle of repose of the landslide dams in Wenchuan earthquake ranges from 28.8°
317 to 44.7°, with an average value of 35.5°(Wang et al., 2013). In the absence of the historical date, the
318 average value proposed by Wang can be used. However, in this way, the difference between the final
319 result and the true value can be about 30% in the worst case. Therefore, on the premise of sufficient
320 disaster relief resources, it is better to make a bad estimate of the repose angle, so as not to make a wrong
321 judgment on the hazard. On the other hand, it is also possible to check the repose angle of the material
322 in advance in landslide prone area, so as to make a quick hazard assessment after the landslide.

323 5.3. Influence of image solution

324 The remote sensing image used in this research is Beijing-1 with a resolution of 0.8m. The pre-landslide
325 DEM is SRTM V3 with a resolution of 30m. As more and more remote sensing data are available, in
326 addition to satellite-based remote sensing platform, small UAV remote sensing platform can also be well
327 applied to this procedure. As different sensors and remote sensing platforms may have different
328 resolutions, we use interpolation to obtain images with different resolutions to explore the appropriate
329 resolution for this procedure (Table 2; Table 3).

330



Input							
Resolution	H_1 (m)	H_0 (m)	H_m (m)	L_m (m)	α (°)	θ (°)	φ (°)
0.8	2944	2860	84	567	30.65	0.11	35.5
5	2946	2861	70	545	28.58	0.10	35.5
15	2943	2856	73	562	29.44	0.09	35.5
30	2956	2862	84	540	29.10	0.16	35.5

331 Table 2 the parameters obtained through different resolution image, where H_1 is the elevation of the
 332 lake level, H_0 is the elevation of the dam bottom, H_m is H_1 minus H_0 , L_m is the length of the
 333 dam that can be observed in the image, α is the slope angle of landslide surface, θ is the inclination
 334 angle of the riverbed and φ is the angle of repose

Resolution	Output		Accuracy
	H (m)	True value H (m)	Error(m)
0.8	2964.2	2967	2.8
5	2964.7	2967	2.3
15	2961.6	2967	5.4
30	2960.5	2967	6.5

335 Table 3 the predicted result of image with different resolutions
 336 As we discussed before, the main parameters in this procedure include the length of the dam that can be
 337 observed, the lake level, the elevation of the dam bottom, the slope angle of landslide surface and the
 338 inclination angle of the riverbed. Obviously, the resolution of the image will affect all of these five (Table
 339 2), but mainly affect the determining of length of the dam that can be observed and the lake level. In
 340 general, the higher the resolution, the more accurate the prediction results obtained. When the resolution
 341 drops from 0.8m to 30m, the error of prediction results changes from 2.8m to 6.5m, as shown in Table 3.
 342 But for the procedure this paper proposed, image with resolution of 5m is sufficient for a good estimate
 343 of the dam height.
 344 There is no doubt that the resolution and quality of DEM data are very important for this procedure.
 345 However, due to the lack of comparative data, this paper does not conduct in-depth discussion on it. For
 346 this part, Dong has had relevant discussions in his research(Dong et al., 2014) for readers' reference.

347 5.4. Other discussion

348 In this study, the formation mechanism of the barrier dam was mainly based on Wu's experiment,
 349 combined with a single remote sensing image and pre-landslide DEM to quickly predict the essential
 350 parameters of the landslide dam hazard. Therefore, a more comprehensive assessment of the reliability of
 351 Wu's theory has also been carried out. It is found that most laws can be applied well, but formula (3) has
 352 greater limitations in fitting the "cut-top" effect. In Wu's experiment, the "cut-top" effect fitting is mainly
 353 determined by the slope angle of landslide surface. Actually, the angle between the riverbed plane and
 354 slope surface of the dam should be determined by its landslide potential energy, landslide length, and



355 landslide angle(Grasselli et al., 2000; Xu et al., 2013; Iverson et al., 2015). In addition to the slope angle
356 of landslide surface, the length of the landslide and potential energy are equally important. In Wu's
357 formula, only the slope angle of landslide surface is considered, so more experiments are needed to
358 improve the fitting.

359 As there is not enough theoretical research to support the prediction of the lowest elevation of the dam
360 crest, the method proposed in this paper still has certain limitations. In addition, the mechanism of the
361 relationship between the highest elevation of the dam crest and the lowest elevation of the dam crest is
362 not clear. In most cases, when it comes to the height of a barrier lake, usually only the highest or lowest
363 elevation is recorded, resulting in fewer complete records of both parameters. As the recording in most
364 cases is not completed, only a small number of cases are used to carry out the fitting. Therefore, this
365 aspect still needs more work and related research to support relevant predictions.
366

367 6. Conclusion

368 This research proposes a procedure based on a single remote sensing image to predict the height of the
369 dam crest and rapidly assess the hazard. With the after-landslide remote sensing image, it only takes no
370 more than one human hour to complete the whole procedure. Compared with Dong's procedure(Dong et
371 al., 2014), this method only requires only one single remote sensing image and has a wider applicability.
372 In view of the large topographic changes in the landslide area, a more reasonable method of using the
373 pre-landslide DEM is proposed. Even the use of poor-quality DEM can complete the relevant prediction
374 and hazard assessment. In the case of Baige Landslide Dam, by extracting the barrier lake surface
375 elevation and determining the bottom elevation of the dam, the prediction of the highest elevation of the
376 dam crest is completed, and the difference between the predicted results and the measured data is within
377 3m. Since the lowest point of the dam crest determines the potential maximum volume of the barrier lake,
378 we based on historical records find that the height of the highest point and the lowest point of the landslide
379 dam crest basically conforms to the linear relationship. The relationship is expressed as a formula (8)
380 through unary fitting. The prediction result of the lowest elevation of the top of the Baige Landslide Dam
381 is 2964.2m, which is consistent with the field measurement results, 2967m. Based on the empirical
382 formula, the potential maximum flood peak of the dam break without treatment is predicted, which is
383 basically consistent with the prediction of a more sophisticated model(Zhang et al., 2019; Chen et al.,
384 2020, 2021; Tian et al., 2020).

385 In the discussion part, the sensitivity of the parameters used in this method is analyzed, and it is found
386 that the repose angle of the landslide material can affect the prediction result up to 30%. Therefore, the
387 repose angle should be carefully determined when using this procedure for related applications. Finally,
388 through experiment with different resolutions of remote sensing images, we find that as the resolution
389 becomes lower, the accuracy of this method decreases. The resolution of 5m and above is a reasonable
390 range for applying this method, otherwise it will be difficult to distinguish the dam body and the water



391 boundary.

392 **Data availability**

393 The data are available from the authors upon request.

394 **Author Contributions**

395 WJZ designed the experiments, and YZ carried them out. SXW and FTW gave some very important
396 suggestions on basic knowledge of landslide dams. LTW, WLL, ZQ and JFZ helped to operate the whole
397 procedure. QG, ZQW helped with some figures, and YBX provided some remote sensing images. FTW
398 prepared the manuscript with contributions from all co-authors.

399 **Competing interests**

400 The authors declare that they have no conflict of interest.

401 **Acknowledgements**

402 The authors acknowledge the support from the National Key R&D Program of China under Grant
403 2017YFB0504101 and Grant 2021YFB3901201.

404 **Financial support**

405 This research has been supported by the National Key R&D Program of China under Grant
406 2017YFB0504101 and Grant 2021YFB3901201.

407
408



409 Reference

- 410 Adams, J.: Earthquake-dammed lakes in New Zealand, 9, 215–219, 1981.
- 411 Ayalew, L. and Yamagishi, H.: The application of GIS-based logistic regression for landslide
412 susceptibility mapping in the Kakuda-Yahiko Mountains, Central Japan, *Geomorphology*, 65, 15–31,
413 <https://doi.org/10.1016/j.geomorph.2004.06.010>, 2005.
- 414 Braun, A., Cuomo, S., Petrosino, S., Wang, X., and Zhang, L.: Numerical SPH analysis of debris flow
415 run-out and related river damming scenarios for a local case study in SW China, *Landslides*, 15, 535–
416 550, <https://doi.org/10.1007/s10346-017-0885-9>, 2018.
- 417 Briaud, J.-L.: Case Histories in Soil and Rock Erosion: Woodrow Wilson Bridge, Brazos River Meander,
418 Normandy Cliffs, and New Orleans Levees, 134, 1425–1447, [https://doi.org/10.1061/\(ASCE\)1090-0241\(2008\)134:10\(1425\)](https://doi.org/10.1061/(ASCE)1090-0241(2008)134:10(1425)), 2008.
- 420 Canuti, P., Casagli, N., Ermini, L., Fanti, R., and Farina, P.: Landslide activity as a geoinicator in Italy:
421 significance and new perspectives from remote sensing, *Environ. Geol.*, 45, 907–919,
422 <https://doi.org/10.1007/s00254-003-0952-5>, 2004.
- 423 Chen, C.-Y., Chen, T.-C., Yu, F.-C., and Hung, F.-Y.: A landslide dam breach induced debris flow – a
424 case study on downstream hazard areas delineation, *Env Geol*, 47, 91–101,
425 <https://doi.org/10.1007/s00254-004-1137-6>, 2004.
- 426 Chen, X. and Lu: Geomatics-based Method Research on Capacity Calculation of Quake Lake, 2008.
- 427 Chen, Z., Chen, S., and Wang, L.: Back analysis of the breach flood of the 11.03 Baige barrier lake at
428 the Upper Jinsha River, 2020.
- 429 Chen, Z., Zhou, H., Ye, F., Liu, B., and Fu, W.: The characteristics, induced factors, and formation
430 mechanism of the 2018 Baige landslide in Jinsha River, Southwest China, *Catena*, 203, 105337,
431 <https://doi.org/10.1016/j.catena.2021.105337>, 2021.
- 432 Costa, J. E. and Schuster, R. L.: The formation and failure of natural dams, 100, 1054–1068,
433 [https://doi.org/10.1130/0016-7606\(1988\)100<1054:TFAFON>2.3.CO;2](https://doi.org/10.1130/0016-7606(1988)100<1054:TFAFON>2.3.CO;2), 1988.
- 434 Costa, J. E. and Schuster, R. L.: Documented historical landslide dams from around the world,
435 Documented historical landslide dams from around the world, U.S. Geological Survey, Vancouver, WA,
436 <https://doi.org/10.3133/ofr91239>, 1991.
- 437 Cui, P., Zhu, Y., Han, Y., Chen, X., and Zhuang, J.: The 12 May Wenchuan earthquake-induced landslide
438 lakes: distribution and preliminary risk evaluation, *Landslides*, 6, 209–223,
439 <https://doi.org/10.1007/s10346-009-0160-9>, 2009.
- 440 Dong, J.-J., Tung, Y.-H., Chen, C.-C., Liao, J.-J., and Pan, Y.-W.: Logistic regression model for
441 predicting the failure probability of a landslide dam, *Engineering Geology*, 117, 52–61,
442 <https://doi.org/10.1016/j.enggeo.2010.10.004>, 2011.
- 443 Dong, J.-J., Lai, P.-J., Chang, C.-P., Yang, S.-H., Yeh, K.-C., Liao, J.-J., and Pan, Y.-W.: Deriving
444 landslide dam geometry from remote sensing images for the rapid assessment of critical parameters
445 related to dam-breach hazards, *Landslides*, 11, 93–105, <https://doi.org/10.1007/s10346-012-0375-z>,
446 2014.
- 447 Ermini, L. and Casagli, N.: Prediction of the behaviour of landslide dams using a geomorphological
448 dimensionless index, 28, 31–47, <https://doi.org/10.1002/esp.424>, 2003.



- 449 Fan, X., van Westen, C. J., Xu, Q., Gorum, T., and Dai, F.: Analysis of landslide dams induced by the
450 2008 Wenchuan earthquake, *Journal of Asian Earth Sciences*, 57, 25–37,
451 <https://doi.org/10.1016/j.jseaes.2012.06.002>, 2012.
- 452 Fan, X., Dufresne, A., Siva Subramanian, S., Strom, A., Hermanns, R., Tacconi Stefanelli, C., Hewitt,
453 K., Yunus, A. P., Dunning, S., Capra, L., Geertsema, M., Miller, B., Casagli, N., Jansen, J. D., and Xu,
454 Q.: The formation and impact of landslide dams – State of the art, *Earth-Science Reviews*, 203, 103116,
455 <https://doi.org/10.1016/j.earscirev.2020.103116>, 2020.
- 456 Fan, X., Dufresne, A., and Whiteley, J.: Recent technological and methodological advances for the
457 investigation of landslide dams, 218, 103646, <https://doi.org/10.1016/j.earscirev.2021.103646>, 2021.
- 458 Grasselli, Y., Herrmann, H. J., Oron, G., and Zapperi, S.: Effect of impact energy on the shape of granular
459 heaps, *GM*, 2, 97–100, <https://doi.org/10.1007/s100350050039>, 2000.
- 460 Iverson, R. M., George, D. L., Allstadt, K., Reid, M. E., Collins, B. D., Vallance, J. W., Schilling, S. P.,
461 Godt, J. W., Cannon, C. M., and Magirl, C. S.: Landslide mobility and hazards: implications of the 2014
462 Oso disaster, 2015.
- 463 Li, H., Qi, S., Chen, H., Liao, H., Cui, Y., and Zhou, J.: Mass movement and formation process analysis
464 of the two sequential landslide dam events in Jinsha River, Southwest China, *Landslides*, 16, 2247–2258,
465 <https://doi.org/10.1007/s10346-019-01254-z>, 2019.
- 466 Li, T. C., Schuster, R. L., and Wu, J. S.: Landslide dams in south-central China, 1986.
- 467 Mora Castro, S.: The 1992 Río Toro landslide dam, Costa Rica, *Landslide News*, 1993.
- 468 Morgenstern, R., Massey, C., Rosser, B., and Archibald, G.: *Landslide Dam Hazards: Assessing Their
469 Formation, Failure Modes, Longevity and Downstream Impacts*, 2021.
- 470 Peng, M. and Zhang, L. M.: Breaching parameters of landslide dams, *Landslides*, 9, 13–31,
471 <https://doi.org/10.1007/s10346-011-0271-y>, 2012.
- 472 Ruan, H., Chen, H., Wang, T., Chen, J., and Li, H.: Modeling Flood Peak Discharge Caused by
473 Overtopping Failure of a Landslide Dam, 13, 921, <https://doi.org/10.3390/w13070921>, 2021.
- 474 Shen, D., Shi, Z., Peng, M., Zhang, L., and Jiang, M.: Longevity analysis of landslide dams, 17, 2020.
- 475 Shi, Z., Ma, X., and Peng, M.: STATISTICAL ANALYSIS AND EFFICIENT DAM BURST
476 MODELLING OF LANDSLIDE DAMS BASED ON A LARGE-SCALE DATABASE, 33, 1780–1790,
477 2014.
- 478 Tian, S., Chen, N., Wu, H., Yang, C., Zhong, Z., and Rahman, M.: New insights into the occurrence of
479 the Baige landslide along the Jinsha River in Tibet, *Landslides*, 17, 1207–1216,
480 <https://doi.org/10.1007/s10346-020-01351-4>, 2020.
- 481 Walder, J. S. and OConnor, J. E.: Methods for predicting peak discharge of floods caused by failure of
482 natural and constructed earthen dams, *Water Resour. Res.*, 33, 2337–2348,
483 <https://doi.org/10.1029/97WR01616>, 1997.
- 484 Wang, J.-J., Zhao, D., Liang, Y., and Wen, H.-B.: Angle of repose of landslide debris deposits induced
485 by 2008 Sichuan Earthquake, *Eng. Geol.*, 156, 103–110, <https://doi.org/10.1016/j.enggeo.2013.01.021>,
486 2013.
- 487 Wang, Z. H. and Lu, J. T.: Satellite monitoring of the Yigong landslide in Tibet, China, in: *Earth
488 Observing Systems VII*, Bellingham, 34–38, <https://doi.org/10.1117/12.453739>, 2002.
- 489 Wu, H., Nian, T., Chen, G., Zhao, W., and Li, D.: Laboratory-scale investigation of the 3-D geometry of
490 landslide dams in a U-shaped valley, *Engineering Geology*, 265, 105428,



- 491 <https://doi.org/10.1016/j.enggeo.2019.105428>, 2020.
- 492 Xu, W.-J., Xu, Q., and Wang, Y.-J.: The mechanism of high-speed motion and damming of the
493 Tangjiashan landslide, *Eng. Geol.*, 157, 8–20, <https://doi.org/10.1016/j.enggeo.2013.01.020>, 2013.
- 494 Yang, S.-H., Pan, Y.-W., Dong, J.-J., Yeh, K.-C., and Liao, J.-J.: A systematic approach for the
495 assessment of flooding hazard and risk associated with a landslide dam, *Nat Hazards*, 65, 41–62,
496 <https://doi.org/10.1007/s11069-012-0344-9>, 2013.
- 497 Yunjian, G., Siyuan, Z., Jianhui, D., Zhiqiu, Y., and Mahfuzur, R.: Flood assessment and early warning
498 of the reoccurrence of river blockage at the Baige landslide, *J. Geogr. Sci.*, 31, 1694–1712,
499 <https://doi.org/10.1007/s11442-021-1918-9>, 2021.
- 500 Zhang, L., Xiao, T., He, J., and Chen, C.: Erosion-based analysis of breaching of Baige landslide dams
501 on the Jinsha River, China, in 2018, 2019.
- 502 Zhong, Q. M., Chen, S. S., Mei, S. A., and Cao, W.: Numerical simulation of landslide dam breaching
503 due to overtopping, *Landslides*, 15, 1183–1192, <https://doi.org/10.1007/s10346-017-0935-3>, 2018.
- 504 Zhou, J., Cui, P., and Hao, M.: Comprehensive analyses of the initiation and entrainment processes of
505 the 2000 Yigong catastrophic landslide in Tibet, China, *Landslides*, 13, 39–54,
506 <https://doi.org/10.1007/s10346-014-0553-2>, 2016.
- 507